Journal of Environmental Chemical Engineering 12 (2024) 113154

Contents lists available at ScienceDirect

Journal of Environmental Chemical Engineering

journal homepage: www.elsevier.com/locate/jece

Novel 3D electro-Fenton reactor based on a catalytic packed bed reactor of perovskite/carbon microelectrodes for the removal of carbamazepine in wastewater

A. Cruz del Álamo [a,*], A. Puga [b], C.M. Dias Soares [b], M.I. Pariente [a], M. Pazos [c], R. Molina [a], M.A. Sanromán [c], F. Martínez [a,d], C. Delerue-Matos [b]

[a] Department of Chemical and Environmental Technology, ESCET, Rey Juan Carlos University, Madrid, Móstoles 28933, Spain
[b] REQUIMTE-LAQV, Instituto Superior de Engenharia do Porto, Instituto Politécnico do Porto, Rua Dr. António Bernardino de Almeida, 431, Porto 4249-015, Portugal
[c] CINTECX, Universidade de Vigo, Department of Chemical Engineering, Campus Universitario As Lagoas–Marcosende, Vigo E-36310, Spain
[d] Instituro de Tecnología para la sostenibilidad, Rey Juan Carlos University, Madrid, Spain

ARTICLE INFO

Keywords:
Perovskite
Carbon black
Microelectrodes
Packed bed
Electro-Fenton
Carbamazepine

ABSTRACT

This presents the efficacy of a 3D-ElectroFenton (3D-EF) reactor with active perovskite/carbon black/PTFE microelectrodes for the removal of carbamazepine (CZP) present in wastewater. Incorporating particle microelectrodes in the reactor enhanced the electron transfer and improved the electrocatalytic efficiency, leading to a more effective CZP removal. The optimal operational conditions were meticulously determined, including current intensity (0.05 – 0.3 A) and particle loading (0 – 1.5 g), to optimize the process and minimize energy consumption. The findings reveal that a current intensity of 0.2 A was the most effective, achieving 90% of CZP removal in 60 min and 3.86 kWh/mg of CZP. A higher current intensity of 0.3 A significantly increased the energy consumption (6.02 kWh/mg of CZP) for a total and faster CZP removal. The 3D-EF reactor was also operated continuously with ultrapure water and real urban wastewater fortified with CZP. A remarkable 62% CZP removal after 96 h on continuous operation was achieved with urban wastewater. Physicochemical and electrochemical characterization of microelectrodes demonstrated their high mechanical integrity and chemical stability. Our study underscores the potential of a 3D-EF system as a promising advanced oxidation process to address the continuous removal of antidepressant carbamazepine as one of the more resistant micropollutants of emerging concern in wastewater treatment, offering hope for a more efficient and sustainable future.

1. Introduction

Electrochemical advanced oxidation processes (EAOPs) have appeared as a valid solution to eliminate toxic and persistent micropollutants, which are refractory to conventional wastewater treatments [1,2]. Among them, electro-Fenton (EF) stands out as a highly effective and versatile "green" technique [3–5]. This treatment consists of the "*in situ*" production of hydroxyl radical ($OH^{\bullet}$, Eq. 1) by the addition of a metallic Fenton-like catalyst (usually iron, Eq. 2), that is highly oxidising [6].

$$H_2O_2 \rightarrow OH^{\bullet} + OH^{-} \quad (1)$$

$$Fe^{2+} + H_2O_2 \rightarrow Fe^{3+} + OH^{\bullet} + OH^{-} \quad (2)$$

At the outset, electro-Fenton (EF) was conducted under acidic conditions at approximately pH 3, employing a homogeneous catalyst, typically iron [7]. This approach raised concerns, rendering the process troublesome. On the one hand, iron in a homogeneous solution in the aqueous medium makes it impossible to reuse the catalyst. On the other hand, the acidification process does not allow the final solution to be dumped directly into the environment despite the management of eliminating micropollutants [8,9]. Both issues make the process less interesting and more difficult to apply at larger scales than in the laboratory. To overcome all these handicaps, several works have proposed to reverse the process towards more ecological systems, such as working at a pH close to neutral by using heterogeneous catalysts that can be efficiently recovered and reused [10–13].

Recently, several authors have considered modifying the

* Corresponding author.
E-mail address: ana.cruz.delalamo@urjc.es (A. Cruz del Álamo).

https://doi.org/10.1016/j.jece.2024.113154
Received 27 December 2023; Received in revised form 20 May 2024; Accepted 22 May 2024
Available online 23 May 2024

electrochemical structure of EF reactors. The electrochemical cell, consisting of an electrode at the anode and another at the cathode, has been modified in terms of the number of electrodes, with the possibility of increasing from two to three electrodes, turning the two-dimensional EF process into a three-dimensional system. In this innovative configuration, the third electrode is positioned between the anode and cathode to (1) expand the effective area to promote a higher H_2O_2 production, breaking the limitation of the low area-volume ratio and mass transfer rate of conventional two electrodes; (2) increase the catalytic reactivity of electrochemical system due to the polarization of particulate microelectrodes and potential regeneration of active metal sites acting as catalysts on their surface; and (3) reduce the energy consumption due to the increase in the efficiency of the process, which in 3D systems is 10–50% higher than in 2D systems[14–18].

As summarised in Table SM1, the third electrode is usually a particulate electrode that is incorporated directly immersed and fluidized in the electrolyte aqueous solution or forming packed bed particles in the circular or rectangular electro-Fenton reactor. The position of particulate microelectrodes is a crucial factor that can affect the effectiveness and performance of the 3D-EF reactor, and it depends on the nature of the material. The fluidised bed offers a high mass transfer with intense mixing and an enormous interfacial zone. However, the packed particle electrodes between the anode and cathode provide a high volume-area ratio, space-time yield, and highest current efficiencies [19]. Moreover, it is worth highlighting that packed bed-like reactors offer an excellent option for working with hydrophobic and low-density materials, which can float on the water surface.

In addition, this new configuration offers different optimisation possibilities, such as incorporating the catalyst in the third electrode. This option makes the process very interesting and ecological, with significant advantages over the traditional experimental configuration [20–22]. As Table SM1 represents, some studies focus on metallic or granular activated carbons as particulate electrode. However, there is a lack of knowledge regarding using a bifunctional material with electroactive properties for H_2O_2 generation and catalytic activity to trigger Fenton reactions as a microelectrode.

Pharmaceutical residues in water have been causing environmental problems for years [23,24], appearing continuously and commonly [25]. Specifically, the family of antidepressants is present in environmental water in significant quantities, worsened by the COVID-19 pandemic [26,27]. While additional data is required to fully understand the impact of micropollutants on aquatic ecosystems and the organisms within them [28,29], it is also evident that the currently available options for their removal are inadequate [30,31]. This is mainly because wastewater treatment plants (WWTPs) struggle to effectively eliminate these substances [30,31]. Among the concerning pharmaceutical residues, carbamazepine (CZP) stands out as a widely used drug, which functions as an anticonvulsant and belongs to the family of antidepressants, specifically tricyclic antidepressants [32]. CZP can be found in surface water, groundwater, treated water, and even drinking water, with concentration values between 0.03 and 11.6 μg/L [33–35]. It is a recalcitrant pollutant that is difficult to eliminate, so it is necessary to improve existing techniques, such as EF, to achieve its total degradation from the aqueous medium. Nowadays, carbamazepine has been studied in numerous works of EAOPs operating in a 2D-electroFenton reactor with a homogeneous [36] and heterogeneous catalyst [37]. Also, Komtchou et al. reported the removal of CZP from spiked municipal wastewater using a discontinuous electro-Fenton process working with a dissolved iron catalyst [38]. However, there is a lack of knowledge about the behaviour of carbamazepine in 3D-electrochemical continuous reactors.

This study evaluated a new three-dimensional EF reactor configuration using bifunctional carbon black (CB)/perovskite particles as third microelectrodes for enhancing the performance of conventional 2D-ElectroFenton systems. As previously reported, the manufactured microelectrodes followed a method free of organic solvents, which was supposed to be an environmentally friendly alternative production [39]. Furthermore, the new 3D-EF configuration represents a step forward in terms of incorporating a bifunctional material as microparticulate electrode, and in the technique that they are packed forming like a bed avoiding the shortcut, which it may be a robust alternative for low-density and floating particulate electrodes.

This new system has been assessed for removing CZP, a frequently detected pharmaceutical in water [25]. CZP's elimination was analysed in a proposed 3D-EF batch cell, working with different operational conditions to optimise the system's performance. The CB/perovskite microelectrodes loadings, air flow rate, and the applied current intensity were studied to analyse their effect on the performance of the system. The feasibility of the proposed reactor to operate under real conditions was validated by working in a continuous mode with two water matrices (ultrapure and WWTP water). Finally, the potential applicability of the technology in real-world scenarios in terms of durability and stability was checked with a long-term continuous experiment and the physicochemical and electrochemical characterization of the microelectrodes.

2. Materials and methods

2.1. Materials

Metallic sources ($Cu(CH_3COO)_2{\cdot}2\,H_2O$, $Mn(NO_3)2{\cdot}4\,H_2O$, $La(NO_3)_3{\cdot}6\,H_2O$) and citric acid for the synthesis of the powdered perovskite material were purchased from Sigma Aldrich (St. Louis, Missouri, USA). Carbon black (CB) and polytetrafluoroethylene (PTFE, 60 wt% dispersion in H_2O) for preparing perovskite/carbon black/PTFE microelectrodes, as well as CZP, used as a model pollutant in the electrocatalytic experiments, was purchased from Sigma -Aldrich, whereas sodium sulfate anhydrous (used as the electrolyte) from Pronalab (Lisboa, Portugal). High-performance liquid chromatography (HPLC) mobile phases were prepared with acetonitrile Chromasolv HPLC grade (≥99.9% purity) from Honeywell (Charlotte, North Carolina, United States), formic acid (99%) from Carlo Erba (Barcelona, Spain) and sulfuric acid from Sigma-Aldrich. All solutions were prepared using Milli-Q grade ultrapure water with a resistivity of 18.2 MΩ.cm (Millipore, Molsheim, France).

2.2. Preparation of perovskite/carbon black/PTFE microelectrodes

2.2.1. Synthesis of powder $LaCu_{0.5}Mn_{0.5}O_3$ perovskite

This material was prepared using the co-precipitation method described by Cruz del Álamo et al. [40], showing remarkable activity and stability in previous work as a bifunctional electrode of an electro-Fenton reactor [39].

2.2.2. Preparation of perovskite/CB/PTFE microelectrodes

Electrodes were prepared according to the method described previously by [39] based on a CB mixture with a 40% wt. of perovskite ($LaCu_{0.5}Mn_{0.5}O_3$), a 12% wt. of PTFE solution (60 wt% in water) as an organic binder and water as a solvent in a 2:1 wt. ratio (carbon black: water). This paste was pressed using a manual press to produce a square flat plate, which was shaped as microelectrodes of an area of 25 mm^2 (5 mm×5 mm) and 2 mm thickness. The microelectrodes were dried at different temperatures in three consecutive steps: at 80 ºC for 2 h, 125 ºC for 1 h, and 250 ºC for 1 h.

2.3. Catalytic test of perovskite microelectrodes in batch 3D-electro-Fenton reactor

The EF reactions were conducted in an undivided batch reactor (see Fig. 1) of acrylic cell (10.5 ×11 x 3 cm) from Cromotema (Vila Nova de Gaia, Portugal). The anode was a Mixed Metal Oxide (MMO) electrode (titanium-coated with RuO_2-IrO_2-TiO_2 of 100 × 20 × 2 mm, UTron-Technology, Youchuang, China). A stainless steel (STS) (AISI-304,

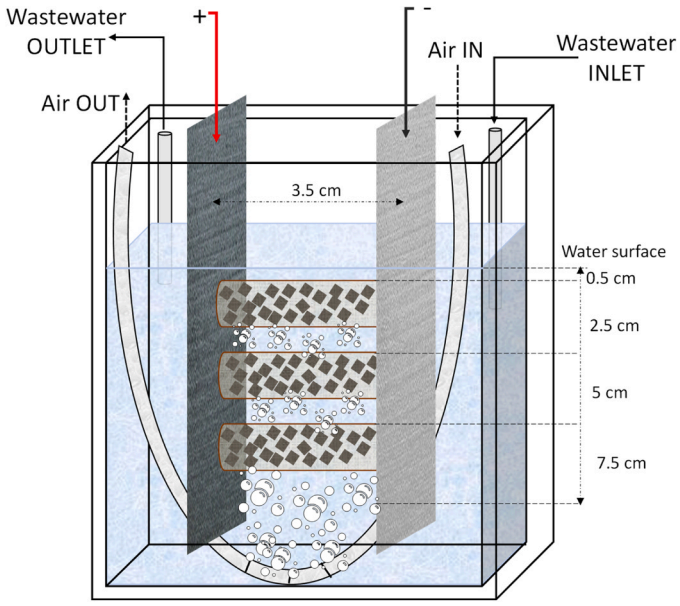

Fig. 1. 3D Electro-Fenton reactor, with MMO anode and STS cathode, and the perovskite microelectrodes at their maximum load studied (1.5 g, divided into three meshes of 0.5 g).

austenitic grade, 100 × 20 × 2 mm) electrode was the cathode. Both electrodes are active with a low oxygen evolution potential, which should limit the anodic oxidation contribution in the overall electrochemical process [41,42]. The rectangular cell design allowed working with a separation gap between electrodes (anode and cathode) of 3.5 cm and a cathodic and anodic submerged active area of 15 cm^2. Microelectrodes were placed between the anode and cathode electrodes in a cylindrical inert high-density polyethylene (HDPE) mesh. These particles are not in direct contact with the commercial electrodes because they are submerged in water. Different loadings of microelectrodes (0.5, 1.0, and 1.5 g) and submergence distances from the water surface (0.5, 2.5, 5.0, and 7.5 cm) were tested. This experimental setup was developed as a new alternative design for floating hydrophobic and low-density carbon-based materials such as perovskite/CB/PTFE microelectrodes that cannot be used as a fluidized bed system in electrochemical chambers.

Electrochemical reactions were carried out using a D.C. power supply, model UTP1305 (UNI-T, Dongguan City, China), featuring adjustable potential (0–32 V) and current (0–5 A) outputs. The mentioned power source constantly supplied a direct current between 50 and 300 mA, monitoring the corresponding potential obtained in the cell. In a typical run, 150 mL of a CZP solution (10 mg/L) containing 10 mM of Na_2SO_4 as a supporting electrolyte was placed in the reactor's chamber, keeping the natural pH of the initial solution (ca. 7 ± 0.5). Air was continuously bubbled in the chamber from the bottom to the top (see Fig. 1) with a continuous airflow between 0 – 0.3 L/min using an ELITE 802 air pump from Hagen (Yorkshire, United Kingdom), ensuring the saturation of the solution. The zero time for the electro-catalytic run was taken once the power supply was turned on. In all the cases, the electrochemical reactor operated at controlled room temperature (22 ± 5 °C).

Specific energy consumption (EC) per mass unit of removed pollutant (CZP) was determined as shown in Eq. (3), where U is the average cell voltage (V), I is the applied current intensity (A), t is the reaction time (h), V is the solution volume (L), and $\Delta C_{pollutant}$ the difference in the CZP concentration (mg/L) before and after the reaction [13].

$$EC\left(\frac{kWh}{mg}\right) = \frac{U \cdot I \cdot t}{V \cdot \Delta Cpollutant} \quad (3)$$

2.4. Continuous 3D-EF reactor working with perovskite microelectrodes for the treatment of CZP in ultrapure water and real wastewater

Finally, the feasibility of the proposed reactor operating under real conditions was validated by working with two water matrices (ultrapure and WWTP water) in the proposed 3D-EF reactor operating in a continuous mode. Two experiments with spiked ultrapure and urban wastewater were carried out to evaluate the efficiency of CZP removal using the optimum conditions fixed previously in batch mode (0.5 g of microelectrodes located at 2.5 cm of submergence, an intensity of 0.2 A and 0.3 L/min of airflow). After that, a long-term experiment using a real urban wastewater spiked with CZP was carried out, keeping the mentioned operational conditions. In this case, four days (96 hours) was considered enough to provide insight into the efficiency and potential applicability of the technology in real-world scenarios.

The urban wastewater was collected from a wastewater treatment plant in the northern region of Portugal, specifically in Paços de Sousa. The collected wastewater had a pH value of 7.59 (Consort C861, Turnhout, Belgium equipped with a Consort SP10B), 1.242 mS/cm of conductivity (Consort C861, Turnhout, Belgium equipped with a conductivity electrode Consort SK10B), and total dissolved solids of 19.0 mg/L. Additionally, the wastewater contained a total nitrogen content of 66.0 mg/L and a chemical oxygen demand of 105 mg O_2/L.

In these experiments, 360 mL of wastewater samples were spiked with 10 mg/L of CZP before treatment in the heterogeneous EF system. In the case of ultrapure water, 10 mM of Na_2SO_4 was added to ensure conductivity and pH of ca. 7 ± 0.5. However, only CZP was added without electrolytes in urban wastewater treatment. Spiked ultrapure and urban wastewater were pumped without recirculation from a reservoir tank to the electrochemical reactor (working volume of 150 mL) using a peristaltic pump (Gilson, Miniplus3, Middleton, USA) with a flow rate of 2 mL/min.

2.5. Analytical techniques for monitoring batch and continuous electro-Fenton treatments

CZP was quantified using high-performance liquid chromatography (HPLC) with a Shimadzu HPLC system (Shimadzu Corporation, Kyoto, Japan), which included an LC-20AB pump, a DGU-20A5 degasser, a SIL-20A automatic injector, a CTO-20AC column oven, and an SPD-M20A diode-array detector. Both LUNA C18 column (particle size 5 μm, 150 × 4.60 mm) connected to a C18 precolumn (particle size 5 μm, 4 × 2.0 mm) as column (particle size 5 μm, 150 × 4.60 mm) and C18 precolumn (particle size 5 μm, 4 × 2.0 mm) from Phenomenex (Torrance, California, USA) were utilized according to previous works [17].

2.6. Physicochemical and electrochemical characterization of perovskite microelectrodes

The physicochemical characterization of perovskite/CB/PTFE microelectrodes surface was performed by X-ray diffraction (XRD) and scanning electron microscopy (SEM) combined with energy dispersive spectrometry (EDS). The presence of carbon and crystalline perovskite particles was measured by an XPert Pro Diffractometer (Philips PW0340/00) using the CuKα radiation. Data were recorded at the 2θ angle ranging from 10° to 90° with steps of 0.04° and 2 s of accumulation each step. However, the superficial distribution of elements on the electrodes was performed by FESEM-EDS using a Phenom XL G2 Desktop SEM equipped with a Silicon Drift EDS detector using an accelerating voltage of 15 kV. The electrical surface resistance of the microelectrode was also measured before and after the long-term experiment using a four-point probe system (Ossila, T2001A3). This technique involves four equally spaced and co-linear probes to make electrical contact with the material.

2.7. Statistical analysis

Statistical analysis was done using IBM SPSS for Windows, version 28 (IBM Corp., Armonk, N.Y.). The dataset's normality was evaluated using the Kolmogorov–Smirnov and Shapiro–Wilk tests. The CZP removal rates were expressed as mean ± standard deviation (n=3). Due to the data's non-normal distribution and the dependent variable's ordinal nature, the Kruskal-Wallis H test was used to identify differences in CPZ removal across various independent groups (see Tables SM2, SM3, SM4, and SM5).

3. Results and discussion

3.1. Catalytic activity of perovskite-microelectrodes in 3D-electro-Fenton reactor

This work proposes an innovative configuration of a 3D-EF reactor in which fabricated perovskite/CB-microparticles are used as the third microelectrode of the system. Thus, the first step to validate this proposal was to evaluate the catalytic properties of these bifunctional microelectrodes for: i) enhancing the H_2O_2 production in the bulk solution of the reactor due to their presence in the cell as a third electrode, thereby improving the transfer of electrons and the H_2O_2 generation and $OH^{\bullet}$ formation (Eqs. 1, 2); and ii) the resulting catalytic decomposition of H_2O_2 into hydroxyl radicals through an EF-like process due to the presence of perovskite ($LaCu_{0.5}Mn_{0.5}O_3$) as a catalytic phase.

In this case, the bifunctional activity of perovskite/CB-microparticles was assessed in the proposed 3D-EF reactor where 0.5 g of the material is in the cylindrical inert mesh between the anode (MMO) and cathode (STS) (see Fig. 1) at 2.5 cm of submergence distance in a solution of 10 mg/L of CZP containing 10 mM of Na_2SO_4 keeping the natural pH (ca. 7 ± 0.5). **Fig. 2** shows the oxidizing CZP removal along the reaction time for a 3D-EF experiment with a direct current of 0.2 A and airflow of 0.3 L/min. Three further control experiments, which were carried out keeping the same conditions of intensity, airflow, and medium properties, are also included in this **Fig. 2** : i) a typical anodic oxidation (same configuration as EF test, but in the absence of catalyst) in the presence of anode and cathode (MMO and STS, respectively), but in the absence of the cylindrical inert mesh and microelectrodes (called 2D); ii) an anodic oxidation test in the presence of the cylindrical inert mesh without microelectrodes (2D+mesh) to analyse the possible adsorption of CZP onto the HDPE material; iii) adsorption (AD-electrodes) experiment in the presence of anodic and cathodic electrode and microelectrodes and non-current electricity and airflow.

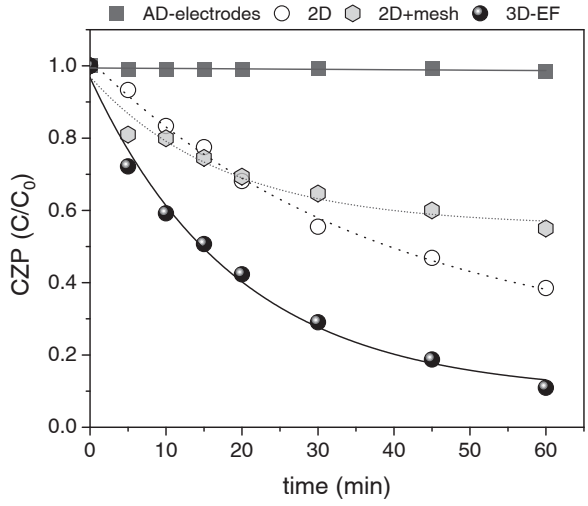

Fig. 2. Catalytic activity of perovskite/CB/PTFE microelectrodes for the removal of CZP in 3D-EF reactor and additional control experiments (2D-reactor, adsorption over electrodes (AD-electrodes) and 2D reaction with adsorption over the cylindrical mesh (2D + AD-mesh)).

As can be seen, the CZP removal by adsorption over the three electrodes (anode, cathode, and microelectrodes) can be discarded as the CZP concentration was not decreased and kept constant during this experiment (AD-electrodes). This may be because perovskite has a low specific surface area [43]. In addition, CZP, due to its pka (pka_1 = 2.3 and pka_2 = 13.9), is neutral in the pH ranges of this study, thus hindering any interaction of surface charges [17]. Considering the results of 2D-EF systems, CZP concentration showed a progressive decay with time for the essay without microelectrodes and cylindrical mesh (2D) and only without microelectrodes (2D+mesh), displaying a removal percentage of 62 and 45%, respectively. As expected, significant removal of CZP was achieved in a typical 2D-electro-Fenton reactor via the catalytic decomposition of electro-generated H_2O_2 to generate oxidizing hydroxyl radicals and anodic oxidation. A similar tendency has been observed in a previous study in which 80% of CZP removal was accomplished after 1 hour working with the same electrodes (MMO as anode and STS as cathode with a submerged active area was 15 cm^2 and interelectrode distance equal to 3.5 cm) in a 2D-electro-Fenton reactor keeping similar operational conditions (10 mg/L of CZP, 10 mM of NaCl, 0.1 A, 0.3 L/min) but working with an acid pH of 5 [17]. Interestingly, a slight decay of the removal rate was observed when the cylindrical mesh was incorporated into the reactor without microelectrodes. This fact may be attributed to increased internal resistance in the cell because the HDPE, which is the mesh's material, is not a conductive element.

Nevertheless, the 3D-EF catalytic run using perovskite/CB-microelectrodes evidenced a remarkable CZP removal compared to the 2D experiments. Results showed that the incorporation of 0.5 g of microelectrodes improved the CZP removal rate from 62% with a 2D-sytem to 90% after 1 h keeping the same conditions of current intensity and airflow. These results demonstrate that incorporating perovskite/CB-microelectrodes enhances the transfer of electrons, delivering higher electrocatalytic efficiency, probably thanks to an intensification of the H_2O_2 production in the bulk solution of the reactor [44,45]. Consequently, the CZP degradation is faster than in a 2D reactor, so the 3D reactor also reduces the system's energy consumption (see Table SM6). Finally, it is important to highlight that the results confirm that the fabricated perovskite/CB microparticles showed a good performance as third microelectrodes, and the proposed EF reactor could be considered a very promising alternative and innovative 3D-configuration.

3.2. Influence of critical variables on the performance of perovskite-microelectrodes in the 3D-electro-Fenton reactor

The influence of some critical parameters that affect the performance and feasibility of a 3D-EF reactor [19] were evaluated, such as the perovskite/CB-microelectrodes loading, the position of microelectrodes packed bed-like in the reactor, the airflow rate, and the current intensity. **Fig. 3** shows the normalized profiles of CZP concentration along the different 3D-EF catalytic batch runs performed for the study of the abovementioned variables.

3.2.1. Effect of perovskite-microelectrodes loadings

In a 3D-EF reactor, the incorporation of particle microelectrodes leads to high electrolytic and electrocatalytic effectiveness in the cell. This is due to its extraordinary expansion of the specific surface area of the electric field, which can improve oxidant electro-production and pollutant removal efficiency. The dosage of particle microelectrodes induces the cost and efficiency of the system. Therefore, finding a suitable and optimal particle dosage is necessary for wastewater treatment, as an excess amount of particle microelectrodes could lead to short-circuiting and decrease removal efficiency [46]. Moreover, an excessive amount of particle microelectrodes placed between the main electrodes (anode and cathode) could limit the electron transfer due to the high resistance they introduce in the cell and generate a shortcut [47].

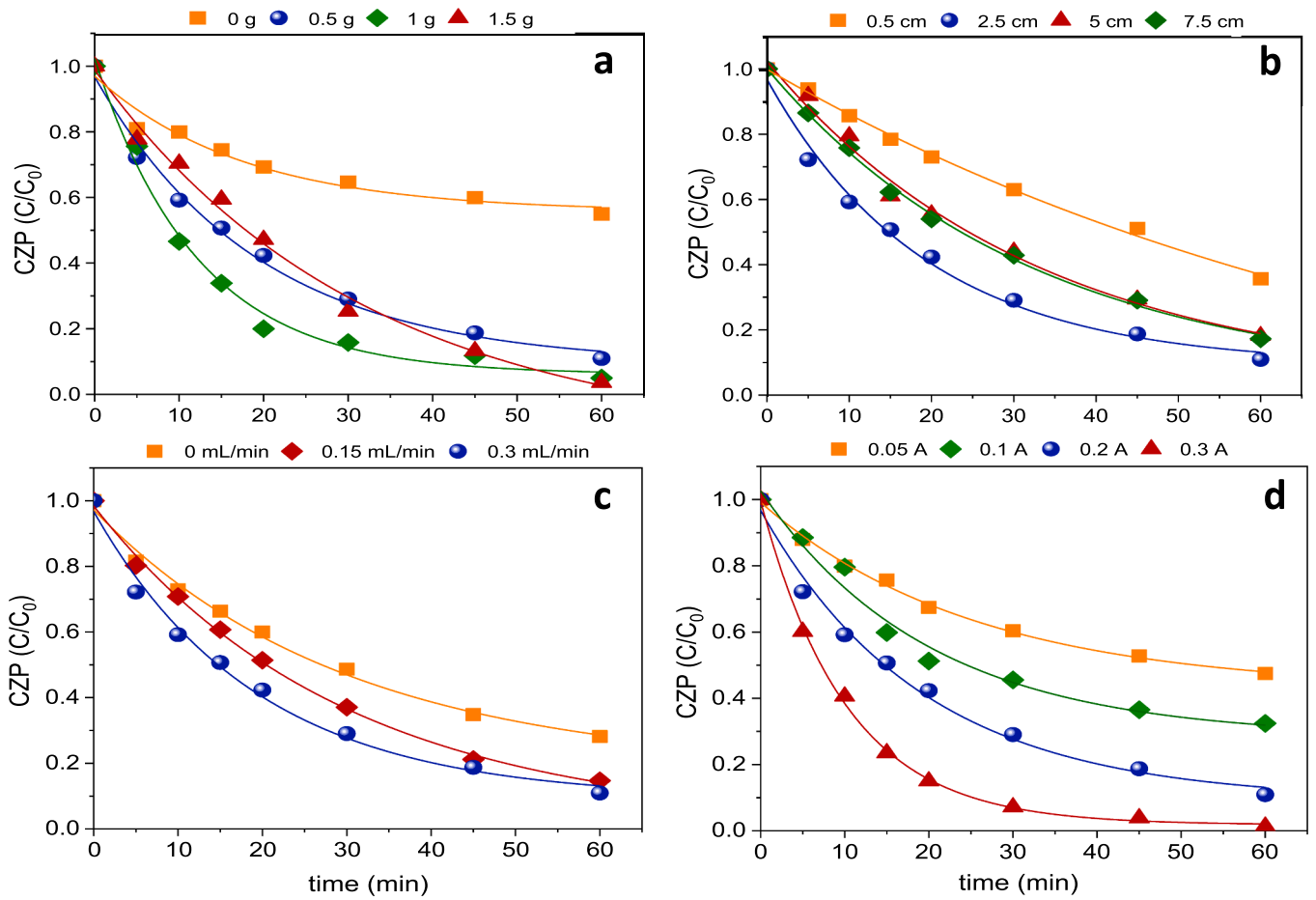

Fig. 3. Catalytic activity of perovskite/CB/PTFE microelectrodes for the removal of CZP in 3D-EF batch reactor: a) microelectrodes loadings, b) microelectrodes packed bed position, c) air flow rate, d) applied current. There was a statistically significant difference in CZP removal between X and Y for $p < 0.05$.

The influence of the microelectrodes dosage in the 3D-system was studied in the range of 0.5–1.5 g, corresponding to a microelectrodes concentration of 3.3–10 g/L. These experiments kept the neutral pH of the solution (10 mg/L of CZP containing 10 mM of Na_2SO_4) with an applied current of 0.2 A while maintaining the airflow at 0.3 L/min. In the experiment with 0.5 g of microelectrodes, only one cylindrical mesh was placed in the cell between the anode and cathode at a submergence depth of 2.5 cm. However, for 1 g of microelectrodes, two cylindrical meshes with 0.5 g each were placed between the main electrodes at 2.5 and 5 cm submergence depths. Finally, to achieve a dosage of 1.5 g in the reactor, three cylindrical meshes (each containing 0.5 g of microelectrodes) were located at submergence depths of 0.5 cm, 2.5 cm, and 5 cm (see Fig. 1). In the control experiment without microelectrodes (0 g), no cylindrical meshes were introduced in the 3D-reactor.

Fig. 3 a shows the CZP removal of the EF experiments performed with the different catalyst loadings, obtaining similar removal rates of CZP (89, 95, 96% for 0.5, 1, and 1.5 g) after 60 minutes for the three tested microelectrodes loadings. The calculation of EC for the different loads has been studied to provide more information about these experiments and determine which is optimal (Table SM6). Once again, like the removals, the results for the three options were similar (3.86, 3.65, and 3.73 kWh/mg CZP for 0.5, 1.0, and 1.5 g of microelectrodes, respectively). Considering these insignificant differences, both in elimination and EC, the lowest dosage of microelectrodes was considered the optimum for the study, as working with a limited amount of material reduces the cost of the process. Moreover, in this case, the highest amount of particle microelectrodes did not imply a significant variability in the resistance of the cell because the monitored voltage followed similar average values working with the three configurations (25.8± 1.1 V for 0.5 g, 23 ± 1.8 V for 1 g, 26.8 ± 1 V for 1.5 g at 0.2 A of applied current). Finally, it is worth highlighting that the experiment without microelectrodes achieved only a CZP removal of 35% after 60 min, exhibiting a tendency that the previous control test without microelectrodes (Fig. 1: 2D+mesh). This confirms the excellent performance of fabricated microelectrodes in enhancing electron transfer, resulting in a higher electrocatalytic efficiency for removing the pollutant.

3.2.2. *Effect of microelectrodes packed bed position*

The position of particulate microelectrodes is a crucial factor that can affect the effectiveness and performance of the 3D-EF reactor. As it mentioned (Table SM1), the literature mainly proposed two configurations: a fluidized bed reactor and a fixed or packed bed reactor. The first offers a high mass transfer with intense mixing and a higher interfacial zone. Nevertheless, the packed particle electrodes without fluidization provide a high volume-area ratio, space-time yield, and highest electric current efficiencies [19]. The selection of an appropriate operation mode is very complicated, and it varies for each 3D-configuration, as it completely depends on the physicochemical properties of the particulate material.

Considering this variable, two experiments were carried out following both reactor types based on the filling pattern of particle microelectrodes. Firstly, 0.5 g of microelectrodes were placed directly between the anode and cathode (without support) in the electrolyte solution (10 mg/L of CZP containing 10 mM of Na_2SO_4) with an applied current of 0.2 A, and the airflow was maintained at 0.3 L/min. The aeration was placed longitudinally in the chamber from the bottom to the top (see Fig. 1) to ensure adequate air circulation. In this case, the fluidized bed reactor setup did not show a correct performance when

working with these manufactured microelectrodes due to CB/perovskite particles floating, limiting the efficiency of the process. Only 25% of CZP removal was accomplished after 60 min because the particles' inadequate mixing in the water medium reduced the electron transfer. However, the CZP removal rate increased to 89% when the same quantity of microelectrodes (0.5 g) was situated forming a packed bed of particles (using the mesh configuration previously described in Fig. 1) at 2.5 cm of submergence. These results showed that a packed bed 3D reactor design is appropriate for working with CB/perovskite microelectrodes.

To increase the knowledge of the study, further experiments with different submergence depths from the water surface (0.5, 2.5, 5.0, and 7.5 cm, Fig. SM1) to evaluate if the proximity with the air source (10 cm depth) has some effect on the removal of the pollutants due to modifying the mass transfer rate. **Fig. 2** b shows the CZP removal of the electro-Fenton experiments performed with 0.5 g of microelectrodes (one cylindrical mesh) at different submergence at 0.2 A and 0.3 L/min of longitudinal airflow from the bottom to the top. Results did not show considerable variations, with similar removal rates at the final time (89, 82, 83% for 2.5, 5.0, and 7.5 cm) but a lower removal rate when working closer to the water surface (64% for 0.5 cm). This reduction in the process effectiveness may be due to the distance from the aeration since the catalyst is not found on the solution's surface either (in this case, the catalyst accumulates outside the solution, sticking to the anode and the cathode). To continue the proposed study on critical variables, a minimum distance of 2.5 cm of submergence was fixed to ensure the maximum efficiency of the process. Furthermore, as shown in **Fig. 2** b, this submergence distance showed a faster CZP removal than the others.

3.2.3. Effect of air flow rate

According to the well-known EF process mechanism, oxygen from the airflow will be reduced at the surface of cathodic and particle electrodes to trigger hydrogen peroxide production [48]. Therefore, the airflow rate directly affects the generation of hydroxyl radicals [42], which is necessary to ensure an aqueous reaction medium is saturated with oxygen and to avoid limitations in the EF process.

In this sense, the aeration of the electrochemical reactor was studied by bubbling longitudinally an airflow of 0.00, 0.15, and 0.30 mL/min, keeping constant the rest of the operational variables (10 mg/L of CZP containing 10 mM of Na_2SO_4 at neutral pH, 0.2 A, and 0.5 g of microelectrodes in a mesh submerged at 2.5 cm). **Fig. 2** c shows the profile of CZP removal along EF essays, obtaining elimination rates of 89% for 0.30 mL/min, 85% for 0.15 mL/min, and only 72% without an air supply. Despite the CZP removal rate at the final reaction time being analogous with 0.30 and 0.15 mL/min, the highest airflow showed a faster pollutant decay. It must be pointed out that the dissolved oxygen naturally present in the aqueous reaction medium was not enough to completely remove the contaminant, which evidenced the requirement for an external air supply to ensure a suitable efficiency of the 3D-EF reactor. Further experiments were carried out working with 0.30 mL/min of airflow to guarantee the constant saturation of the reaction medium, following Eq. 4.

$$\boldsymbol{O_2 + \ 4H^+ + \ 4e^- \rightarrow \ 2H_2O} \quad (4)$$

3.2.4. Effect of the current intensity

The applied current density is considered one of the most influential factors affecting the electrochemical process's effectiveness, performance, and cost [49]. Moreover, in the case of the 3D-EF reactor, particle perovskite/CB/PTFE microelectrodes contribute directly to the electrochemical process of H_2O_2 generation and play a role in the polarization of the microelectrodes. Hence, finding an optimal condition is essential for two reasons: i) to avoid parasitic reactions that occur simultaneously if the system works with an excessive cell voltage, which can reduce the efficiency of the process [49–51], and ii) to optimize the energy consumption of the system, which is crucial to avoid working with higher current densities, as they may lead to a non-scalable process due to increased costs [19].

The effect of the current intensity in the 3D system was studied at fixed values of 0.05, 0.10, 0.20, and 0.30 A, which correspond to current densities of 0.003, 0.006, 0.013, and 0.02 A/cm^2. These experiments were carried out keeping the neutral pH of the CZP solution (10 mg/L of CZP containing 10 mM of Na_2SO_4) with 0.5 g of microelectrodes placed in one cylindrical mesh at 2.5 cm of submergence depth and an airflow of 0.30 L/min. **Fig. 2** d shows the CZP removal of the EF experiments performed with the different currents. As expected, the increase of the applied intensity enhanced the CZP decay, obtaining final degradation rates of 53, 66, 89, and 99% at 0.05, 0.10, 0.20, and 0.30 A, respectively. However, this improvement was significantly less accentuated (10%) from 0.2 to 0.3 A.

The specific energy consumption (EC) per mass unit of removed pollutant (CZP) was calculated for each condition (Table SM6) to consider the main cost for the EF treatment [52] in the selection of the most suitable operational current intensity. These results are lower than the previous values reported in the literature using a 3D-electrochemical reactor for the CZP removal using three different particle electrodes (394 kWh/mg$_{CZP}$ using biochar $<$ 75 μm, 390kWh/mg$_{CZP}$ using biochar of 1–2 mm and 401 kWh/mg$_{CZP}$ using an activated carbon) at similar current densities (0.0067 A/cm^2) and final time of 45 min [17].

Considering CZP removal and EC, a current intensity of 0.20 A was determined to be the best-tested value, ensuring an exceptional efficacy of the process in removing CZP while maintaining a limited energy consumption using the proposed and novel 3D-configuration. In this case, the highest intensity (0.30 A) was discarded because it required double the specific EC compared to 0.20 A (3.86 and 6.02 kWh/mg for 0.2 and 0.3 A, respectively) to achieve only a 10% improvement in CZP removal. This selection has further implications regarding having a system that is more environmentally sustainable and more competitive on the industrial scale because their cost could be reduced.

3.3. Continuous 3D-EF reactor working with perovskite-microelectrodes to treat CZP in ultrapure water and real wastewater

Once the CZP degradation in ultrapure water was evaluated in the 3D-EF reactor under batch mode, preliminary experiments of continuous treatment of 3 hours were performed with CZP spiked ultrapure water and urban wastewater 10 mg/L) using 2 mL/min of feed flow rate, which provide 75 min of hydraulic retention time (HRT). As can be seen from **Fig. 4** a, 65% of the CZP removal rate was achieved after 3 hours of operation. This result is comparable with other electrochemical oxidation process reported in the literature to remove CZP from an ultrapure water matrix in a continuous mode. Li et al. [53] have reported the removal of 90% of CZP in a sequential system using electrochemical peroxidation with peroxymonosulfate (PMS) and a continuous electro-Fenton treatment with cobalt-containing hydrochar after 8 hours with a flowrate of 1 mL/min (HRT of 0.25 min), but with an initial concentration of 50 mg/L in acid (pH 3) ultrapure water and BDD as cathode. In another study with persulfate (PS) activated by a continuous electrochemical process [54], the CZP degradation was completely removed operating with a 6 mL/min (HRT of 17 min) of a 5 mg/L CZP solution in ultrapure water (pH 7 and 50 Mm of Na_2SO_4) after 120 min.

The performance of the 3D-EF reactor with the urban wastewater showed a decrease in the CZP removal rate to 50% (**Fig. 4** a). It must be pointed out that this experiment was performed using the same conditions as the experiment with ultrapure water but without the addition of electrolytes, considering the conductivity of the wastewater. Real urban wastewater is a more complex matrix with an additional organic load and other substrates that can be reactive to the hydroxyl radicals generated during the electro-Fenton process. Furthermore, the experiment was conducted at the natural pH of the wastewater matrix (ca. 7.59 ± 0.50) with no pH change to the optimum acid range so the treated

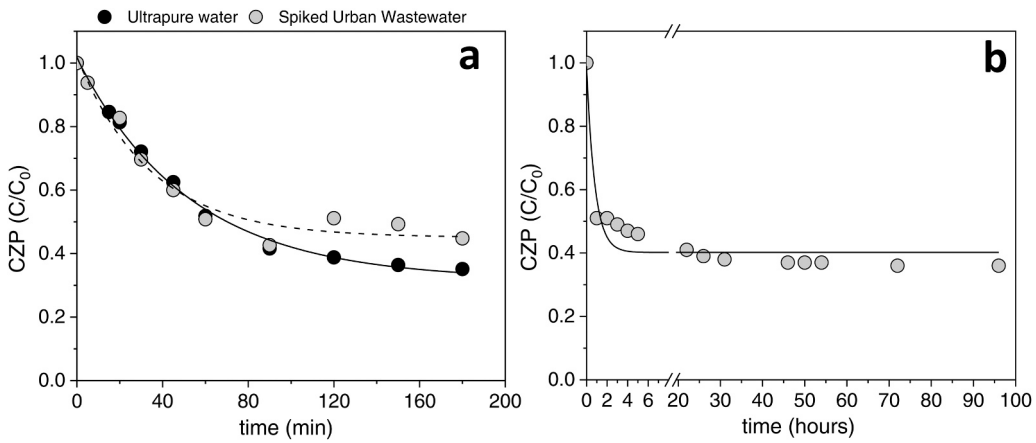

Fig. 4. (a) Preliminary continuous electrochemical experiments of spiked ultrapure and real urban wastewater, (b) long-term continuous experiment of spiked real urban wastewater for 4 days in 3D-Electro-Fenton reactor with perovskite microelectrodes. Reaction conditions: 10 mg/L of initial CZP concentration, 0.5 g of microelectrodes, 2.5 cm of fix-bed position, 0.30 L/min of airflow, 0.20 A and 2 mL/min of wastewater flow rate.

outlet stream could be discharged into the sewer without needing subsequent conditioning pH operation. Zou et al. [55], evaluated the CZP removal of real wastewater and ultrapure water with an initial concentration of 550 μg/L under different voltages and flowrates, showed a more drastic difference (up to 40%) between both matrices, a percentage far from that reached in the present study. The low difference in the CZP removal rate between the ultrapure water and the real wastewater evidence a less critical influence of the wastewater matrix in the 3D electro-Fenton system.

A long-term experiment for treating the CZP spiked wastewater for four days to assess the stability of the 3D electro-Fenton reactor displayed an increase of the CZP elimination at steady state conditions after 24 hours to ca. 62%, which kept constant after 72 hours else (Fig. 4b). This result confirms that the proposed 3D-EF reactor maintains its efficiency in the CZP removal for 96 hours of operation. This fact revealed the stability of the 3D-EF catalytic system using bifunctional particle microelectrodes as potential tertiary treatment for a wastewater treatment plant (WWTP) to remove micropollutants that usually are not eliminated. The performance of the continuous treatment proposed in this work achieves a considerable elimination of the targeted contaminant with a reasonable energy cost.

The physicochemical and electrochemical characterization of the microelectrodes after the long-term continuous experiment was also studied. XRD patterns of initial and used microelectrodes after four days of operation showed non-significant changes (Fig. SM2), maintaining the characteristic spectra of initial carbon-based microelectrodes with an amorphous structure and reflections at 24 and 44° representative of certain graphitic domains [56]. Characteristic peaks of the PTFE binder and crystalline $LaCu_{0.5}Mn_{0.5}O_3$ perovskite [39] were not observed due to the low content of PTFE and small crystalline particles of perovskite on the carbon-based microelectrodes. However, the elemental mapping analysis of two samples of fresh and used microelectrodes made by FESEM-EDS proves the presence of carbon, lanthanum, fluorine, oxygen, and copper on the electrode surface (see Fig. SM3, SM4 and SM5). The quantitative composition of the surface electrode evidenced a high amount of carbon (85 ± 10% wt.) in all the samples, followed by oxygen (15 ± 10% wt.). In minor contribution, fluorine from PTFE and lanthanum and copper from $LaCu_{0.5}Mn_{0.5}O_3$ perovskite were also quantified with non-significant differences between initial and used microelectrodes which seem to indicate that the chemical surface composition was not altered after four days of continuous treatment of urban wastewater spiked with CZP using the 3D electro-Fenton system. The electrical surface resistance of initial and used microelectrodes was also measured by the four-point probe system. Electrochemical perovskite/CB/PTFE electrode characterization has been previously reported [39]. In this case, the electrical surface resistance of microelectrodes increased from values around 1.9 kΩ/m^2 for initial microelectrodes up to 4.2 kΩ/m^2 for the microelectrodes after 96 hours of operation in the 3D- electro-Fenton reactor. This increase in the resistance is probably associated with the fouling of the surface during the treatment of real wastewater [50], but this fact does not seem to be critical to the CZP removal as it keeps constant during the steady state of the 3D electro-Fenton reactor (see Fig. 4(b)). Moreover, it must be noteworthy that microelectrodes maintain their mechanical integrity in 3D-packed bed cells for 96 hours of operation. All these results indicate a promising stability of the microelectrodes, which significantly impact the scalability and sustainability of the technology.

4. Conclusions

Incorporating particle microelectrodes made from perovskite/carbon black in a 3D-EF reactor showed promising results in enhancing the transfer of electrons and achieving higher electrocatalytic efficiency for removing micropollutants, such as CZP. The optimization of operational conditions, including the selection of an appropriate current intensity (0.2 A) and particle dosage (0.5 g), proved to be crucial for maximizing the performance (90% CZP removal in 60 min) and energy efficiency of the electroFenton process. The energy consumption for the optimal conditions in the batch experiments has also been relevant, with only 3.86 kWh/mg of CZP. The continuous operation of the 3D-EF reactor demonstrated its potential for CZP removal, achieving a 62% CZP abatement in spiked real urban wastewater. 3D-EF reactor maintains its efficiency in the CZP removal for 96 h on operation, which revealed the robustness of the proposed 3D electro-Fenton system based on the bifunctional activity of particle microelectrodes for hydrogen peroxide generation and catalytic decomposition to powerful oxidizing hydroxyl radicals. Moreover, microelectrodes kept their physicochemical and mechanical properties after 96 hours without deactivation, which evidences their stability and durability for an actual continuous treatment. A comparison with previous studies underscored the novelty and innovation of the proposed research, as it achieved significantly higher CZP removal rates than other systems working with real water matrices. Overall, the study contributes valuable insights into the continuous electrochemical degradation of CZP, specifically in a 3D-reactor setup, which could pave the way for future more effective and sustainable electroFenton wastewater treatment approaches.

Declaration of Competing Interest

The authors declare that they have no known competing financial

interests or personal relationships that could have appeared to influence the work reported in this paper.

Data availability

Data will be made available on request.

Acknowledgements

This work was supported by projects REQUIMTE/LAQV—UIDB/50006/2020, UIDP/50006/2020, LA/P/0008/2020 and EXPL/BII-BIO/0436/2021 and financed by FCT/Ministério da Ciência, Tecnologia e Ensino Superior (MCTES) through national funds. This work was also supported through the Biodiversa & Water JPI joint call for research proposals under the BiodivRestore ERA-Net COFUND program, BiodivRestore-406DivRestore/0002/2020, and cofunding by FCT, Portugal and Project PCI2022–132941 cofunding by MCIN/AEI/10.13039/501100011033. The authors also wish to thank the program supported by Rey Juan Carlos University (URJC) for postdoctoral international stays of young researchers as well as SLUD4MAT&WATER (PID2021–122883OB-I00) project financed by Ministry of Science and Innovation, and ELECTROCHAR (M2739) URJC-project as an action financed by the Community of Madrid *(Comunidad de Madrid)* in the framework of the multi-annual agreement with the *Universidad Rey Juan Carlos* in its *Programa de Estímulo a la Investigación de Jóvenes Doctores* (Programme to Stimulate Research by Young Doctors). A. Puga acknowledges FCT for the Ph.D. grant (2021.08888.BD).

Appendix A. Supporting information

Supplementary data associated with this article can be found in the online version at doi:10.1016/j.jece.2024.113154.

References

[1] B.L. Phoon, C.C. Ong, M.S. Mohamed Saheed, P.L. Show, J.S. Chang, T.C. Ling, S. S. Lam, J.C. Juan, Conventional and emerging technologies for removal of antibiotics from wastewater, J. Hazard. Mater. *400* (2020) 122961, https://doi.org/10.1016/J.JHAZMAT.2020.122961.

[2] L. Liu, Z. Chen, J. Zhang, D. Shan, Y. Wu, L. Bai, B. Wang, Treatment of industrial dye wastewater and pharmaceutical residue wastewater by advanced oxidation processes and its combination with nanocatalysts: a review, J. Water Process Eng. *42* (2021) 102122, https://doi.org/10.1016/j.jwpe.2021.102122.

[3] J. Meijide, P.S.M. Dunlop, M. Pazos, M.A. Sanromán, Heterogeneous electro-fenton as "green" technology for pharmaceutical removal: a review, Catalysts *11* (2021).

[4] S.A. Ismail, W.L. Ang, A.W. Mohammad, Electro-fenton technology for wastewater treatment: a bibliometric analysis of current research trends, future perspectives and energy consumption analysis, J. Water Process Eng. *40* (2021) 101952, https://doi.org/10.1016/j.jwpe.2021.101952.

[5] P.V. Nidheesh, S.O. Ganiyu, C.A. Martínez-Huitle, E. Mousset, H. Olvera-Vargas, C. Trellu, M. Zhou, M.A. Oturan, Recent advances in electro-fenton process and its emerging applications, Crit. Rev. Environ. Sci. Technol. *53* (2022) 887–913, https://doi.org/10.1080/10643389.2022.2093074.

[6] X. Qin, P. Cao, X. Quan, K. Zhao, S. Chen, H. Yu, Y. Su, Highly efficient hydroxyl radicals production boosted by the atomically dispersed Fe and Co sites for heterogeneous electro-fenton oxidation, Environ. Sci. Technol. (2022), https://doi.org/10.1021/acs.est.2c06981.

[7] L. Martone, M. Minella, C. Minero, F. Sordello, D. Vione, Effective degradation of ibuprofen through an electro-fenton process, in the presence of zero-valent iron (ZVI-EF), J. Clean. Prod. *367* (2022) 132894, https://doi.org/10.1016/j.jclepro.2022.132894.

[8] J.F.J.R. Pesqueira, J. Marugán, M.F.R. Pereira, A.M.T. Silva, Selecting the most environmentally friendly oxidant for UVC degradation of micropollutants in urban wastewater by assessing life cycle impacts: hydrogen peroxide, peroxymonosulfate or persulfate? Sci. Total Environ. *808* (2022) https://doi.org/10.1016/j.scitotenv.2021.152050.

[9] N. Nasrollahi, V. Vatanpour, A. Khataee, Removal of antibiotics from wastewaters by membrane technology: limitations, successes, and future improvements, Sci. Total Environ. *838* (2022) 156010, https://doi.org/10.1016/j.scitotenv.2022.156010.

[10] G. Pan, Z. Sun, Cu-Doped g-C3N4 catalyst with stable Cu0 and Cu+ for enhanced amoxicillin degradation by heterogeneous electro-fenton process at neutral PH, Chemosphere *283* (2021) 131257, https://doi.org/10.1016/j.chemosphere.2021.131257.

[11] J. Liang, Y. Hou, H. Zhu, J. Xiong, W. Huang, Z. Yu, S. Wang, Levofloxacin degradation performance and mechanism in the novel electro-fenton system constructed with vanadium oxide electrodes under neutral PH, Chem. Eng. J. *433* (2022) 133574, https://doi.org/10.1016/j.cej.2021.133574.

[12] A. Puga, E. Rosales, M. Pazos, M.A. Sanromán, Prompt removal of antibiotic by adsorption/electro-fenton degradation using an iron-doped perlite as heterogeneous catalyst, Process Saf. Environ. Prot. *144* (2020) 100–110, https://doi.org/10.1016/j.psep.2020.07.021.

[13] V. Poza-Nogueiras, Á. Moratalla, M. Pazos, Á. Sanromán, C. Sáez, M.A. Rodrigo, Towards a more realistic heterogeneous electro-fenton, J. Electroanal. Chem. *895* (2021) 115475, https://doi.org/10.1016/J.JELECHEM.2021.115475.

[14] H.H. Phan Quang, T.P. Nguyen, D.D. Duc Nguyen, L.T. Ngoc Bao, D.C. Nguyen, V. H. Nguyen, Advanced electro-fenton degradation of a mixture of pharmaceutical and steel industrial wastewater by pallet-activated-carbon using three-dimensional electrode reactor, Chemosphere *297* (2022) 134074, https://doi.org/10.1016/j.chemosphere.2022.134074.

[15] Y. Zhang, Z. Chen, P. Wu, Y. Duan, L. Zhou, Y. Lai, F. Wang, S. Li, Three-dimensional heterogeneous electro-fenton system with a novel catalytic particle electrode for bisphenol a removal, J. Hazard. Mater. *393* (2020) 120448, https://doi.org/10.1016/j.jhazmat.2019.03.067.

[16] C. Zhang, F. Li, R. Wen, H. Zhang, P. Elumalai, Q. Zheng, H. Chen, Y. Yang, M. Huang, G. Ying, Heterogeneous electro–fenton using three–dimension NZVI–BC electrodes for degradation of neonicotinoid wastewater, Water Res. *182* (2020) 115975, https://doi.org/10.1016/j.watres.2020.115975.

[17] L. Correia-Sá, C. Soares, O.M. Freitas, M.M. Moreira, H.P. Nouws, M. Correia, P. Paíga, A.J. Rodrigues, C.M. Oliveira, S.A. Figueiredo, et al., A three-dimensional electrochemical process for the removal of carbamazepine, Appl. Sci. *11* (2021).

[18] H. Xiao, Y. Hao, J. Wu, X. Meng, F. Feng, F. Xu, S. Luo, B. Jiang, Differentiating the reaction mechanism of three-dimensionally electrocatalytic system packed with different particle electrodes: electro-oxidation versus electro-fenton, Chemosphere *325* (2023) 138423, https://doi.org/10.1016/j.chemosphere.2023.138423.

[19] K. GracePavithra, P. Senthil Kumar, V. Jaikumar, P. SundarRajan, A review on three-dimensional eletrochemical systems: analysis of influencing parameters and cleaner approach mechanism for wastewater, Rev. Environ. Sci. Bio/Technol. *19* (2020) 873–896, https://doi.org/10.1007/s11157-020-09550-0.

[20] H. Ghanbarlou, B. Nasernejad, M. Nikbakht Fini, M.E. Simonsen, J. Muff, Synthesis of an iron-graphene based particle electrode for pesticide removal in three-dimensional heterogeneous electro-fenton water treatment system, Chem. Eng. J. *395* (2020) 125025, https://doi.org/10.1016/j.cej.2020.125025.

[21] Y. Zheng, S. Qiu, F. Deng, Y. Zhu, G. Li, F. Ma, Three-dimensional electro-fenton system with iron foam as particle electrode for folic acid wastewater pretreatment, Sep. Purif. Technol. *224* (2019) 463–474, https://doi.org/10.1016/j.seppur.2019.05.054.

[22] X. Meng, K. Li, Z. Zhao, Y. Li, Q. Yang, B. Jiang, A PH self-regulated three-dimensional electro-fenton system with a bifunctional fe-cu-c particle electrode: high degradation performance, wide working ph and good anti-scaling ability, Sep. Purif. Technol. *298* (2022) 121672, https://doi.org/10.1016/j.seppur.2022.121672.

[23] S. Khan, M. Naushad, M. Govarthanan, J. Iqbal, S.M. Alfadul, Emerging contaminants of high concern for the environment: current trends and future research, Environ. Res. *207* (2022) 112609, https://doi.org/10.1016/j.envres.2021.112609.

[24] T.K. Kasonga, M.A.A. Coetzee, I. Kamika, V.M. Ngole-Jeme, M.N. Benteke Momba, Endocrine-Disruptive Chemicals as Contaminants of Emerging Concern in Wastewater and Surface Water: A Review, J. Environ. Manag. *277* (2021) 111485, https://doi.org/10.1016/j.jenvman.2020.111485.

[25] P. Paíga, M. Correia, M.J. Fernandes, A. Silva, M. Carvalho, J. Vieira, S. Jorge, J. G. Silva, C. Freire, C. Delerue-Matos, Assessment of 83 pharmaceuticals in WWTP influent and effluent samples by UHPLC-MS/MS: hourly variation, Sci. Total Environ. *648* (2019) 582–600, https://doi.org/10.1016/j.scitotenv.2018.08.129.

[26] E. Yavuz-Guzel, A. Atasoy, İ.E. Gören, N. Daglioglu, Impact of COVID- 19 pandemic on antidepressants consumptions by wastewater analysis in Turkey, Sci. Total Environ. *838* (2022), https://doi.org/10.1016/j.scitotenv.2022.155916.

[27] E.M. Melchor-Martínez, M.G. Jiménez-Rodríguez, M. Martínez-Ruiz, S.A. Peña-Benavides, H.M.N. Iqbal, R. Parra-Saldívar, J.E. Sosa-Hernández, Antidepressants surveillance in wastewater: overview extraction and detection, Case Stud. Chem. Environ. Eng. *3* (2021), https://doi.org/10.1016/j.cscee.2020.100074.

[28] E. Drakvik, R. Altenburger, Y. Aoki, T. Backhaus, T. Bahadori, R. Barouki, W. Brack, M.T.D. Cronin, B. Demeneix, S. Hougaard Bennekou, et al., Statement on advancing the assessment of chemical mixtures and their risks for human health and the environment, Environ. Int. *134* (2020), https://doi.org/10.1016/j.envint.2019.105267.

[29] M. Bilal, S. Mehmood, T. Rasheed, H.M.N. Iqbal, Antibiotics traces in the aquatic environment: persistence and adverse environmental impact, Curr. Opin. Environ. Sci. Health *13* (2020) 68–74, https://doi.org/10.1016/j.coesh.2019.11.005.

[30] M. Scheurer, A. Sandholzer, T. Schnabel, S. Schneider-Werres, M. Schaffer, H. Börnick, S. Beier, Persistent and mobile organic chemicals in water resources: occurrence and removal options for water utilities, Water Supply *22* (2022) 1575–1592, https://doi.org/10.2166/ws.2021.336.

[31] K.M. Kanama, A.P. Daso, L. Mpenyana-Monyatsi, M.A.A. Coetzee, Assessment of pharmaceuticals, personal care products, and hormones in wastewater treatment plants receiving inflows from health facilities in North West Province, South Africa, J. Toxicol. *2018* (2018), https://doi.org/10.1155/2018/3751930.

[32] J. Chen, L. Bai, Y. He, A possible case of carbamazepine-induced renal phospholipidosis mimicking fabry disease, Clin. Exp. Nephrol. *26* (2022) 303–304, https://doi.org/10.1007/s10157-021-02172-y.

[33] S. García-Medina, M. Galar-Martínez, L.M. Gómez-Oliván, R.M. del C. Torres-Bezaury, H. Islas-Flores, E. Gasca-Pérez, The relationship between cyto-genotoxic damage and oxidative stress produced by emerging pollutants on a bioindicator organism (allium cepa): the carbamazepine case, Chemosphere *253* (2020), https://doi.org/10.1016/j.chemosphere.2020.126675.

[34] Y. Han, M. Ma, Y. Oda, K. Rao, Z. Wang, R. Yang, Y. Liu, Insight into the generation of toxic products during chloramination of carbamazepine: kinetics, transformation pathway and toxicity, Sci. Total Environ. *679* (2019) 221–228, https://doi.org/10.1016/j.scitotenv.2019.04.423.

[35] M.I. Pariente, Y. Segura, S. Álvarez-Torrellas, J.A. Casas, Z.M. de Pedro, E. Diaz, J. García, M.J. López-Muñoz, J. Marugán, A.F. Mohedano, et al., Critical review of technologies for the on-site treatment of hospital wastewater: from conventional to combined advanced processes, J. Environ. Manag. *320* (2022) 115769, https://doi.org/10.1016/j.jenvman.2022.115769.

[36] G. Song, X. Du, Y. Zheng, P. Su, Y. Tang, M. Zhou, A novel electro-fenton process coupled with sulfite: enhanced Fe(3+) reduction and TOC removal, J. Hazard. Mater. *422* (2022) 126888, https://doi.org/10.1016/j.jhazmat.2021.126888.

[37] J. Guo, G. Song, M. Zhou, Highly dispersed FeN-CNTs heterogeneous electro-fenton catalyst for carbamazepine removal with low fe leaching at wide PH, Chem. Eng. J. *474* (2023) 145681, https://doi.org/10.1016/j.cej.2023.145681.

[38] S. Komtchou, A. Dirany, P. Drogui, A. Bermond, Removal of carbamazepine from spiked municipal wastewater using electro-fenton process, Environ. Sci. Pollut. Res. *22* (2015) 11513–11525, https://doi.org/10.1007/s11356-015-4345-6.

[39] A. Cruz del Álamo, A. Puga, M.I. Pariente, E. Rosales, R. Molina, M. Pazos, F. Martínez, M.A. Sanromán, Activity and stability of bifunctional perovskite/carbon-based electrodes for the removal of antipyrine by electro-fenton process, Chemosphere (2023) 138858, https://doi.org/10.1016/J.CHEMOSPHERE.2023.138858.

[40] A.C. del Álamo, C. González, M.I. Pariente, R. Molina, F. Martínez, Fenton-like catalyst based on a reticulated porous perovskite material: activity and stability for the on-site removal of pharmaceutical micropollutans in a hospital wastewater, Chem. Eng. J. *401* (2020) 126113, https://doi.org/10.1016/j.cej.2020.126113.

[41] M. Panizza, G. Cerisola, Direct and mediated anodic oxidation of organic pollutants, Chem. Rev. *109* (2009) 6541–6569, https://doi.org/10.1021/cr9001319.

[42] E. Brillas, C.A. Martínez-Huitle, Decontamination of wastewaters containing synthetic organic dyes by electrochemical methods. an updated review, Appl. Catal. B: Environ. *166–167* (2015) 603–643, https://doi.org/10.1016/J.APCATB.2014.11.016.

[43] L. Huang, X. Huang, J. Yan, Y. Liu, H. Jiang, H. Zhang, J. Tang, Q. Liu, Research progresses on the application of perovskite in adsorption and photocatalytic removal of water pollutants, J. Hazard. Mater. *442* (2023) 130024, https://doi.org/10.1016/j.jhazmat.2022.130024.

[44] L. Jing, C. Tang, Q. Tian, T. Liu, S. Ye, P. Su, Y. Zheng, J. Liu, Mesoscale diffusion enhancement of carbon-bowl-shaped nanoreactor toward high-performance electrochemical H2O2production, ACS Appl. Mater. Interfaces *13* (2021) 39763–39771, https://doi.org/10.1021/acsami.1c11765.

[45] P. Cao, X. Quan, X. Nie, K. Zhao, Y. Liu, S. Chen, H. Yu, J.G. Chen, Metal single-site catalyst design for electrocatalytic production of hydrogen peroxide at industrial-relevant currents, Nat. Commun. *14* (2023) 1–12, https://doi.org/10.1038/s41467-023-35839-z.

[46] L. Wang, Y. Hu, P. Li, Y. Zhang, Q. Yan, Y. Zhao, Electrochemical treatment of industrial wastewater using a novel layer-upon-layer bipolar electrode system (NLBPEs), Chem. Eng. J. *215–216* (2013) 157–161, https://doi.org/10.1016/j.cej.2012.11.026.

[47] J. Li, J. Yan, G. Yao, Y. Zhang, X. Li, B. Lai, Improving the degradation of atrazine in the three-dimensional (3D) electrochemical process using CuFe2O4 as both particle electrode and catalyst for persulfate activation, Chem. Eng. J. *361* (2019) 1317–1332, https://doi.org/10.1016/j.cej.2018.12.144.

[48] A. Cruz del Alamo, R. Zou, M.I. Pariente, R. Molina, F. Martínez, Y. Zhang, Catalytic activity of LaCu0.5Mn0.5O3 perovskite at circumneutral/basic PH conditions in electro-fenton processes, Catal. Today (2020) 1–6, https://doi.org/10.1016/j.cattod.2020.03.027.

[49] B.A. Marinho, L. Suhadolnik, B. Likozar, M. Huš, Ž. Marinko, M. Čeh, Photocatalytic, electrocatalytic and photoelectrocatalytic degradation of pharmaceuticals in aqueous media: analytical methods, mechanisms, simulations, catalysts and reactors, J. Clean. Prod. *343* (2022) 131061, https://doi.org/10.1016/j.jclepro.2022.131061.

[50] A. Cruz del Álamo, R. Zou, M.I. Pariente, R. Molina, F. Martínez, Y. Zhang, Catalytic activity of LaCu0.5Mn0.5O3 perovskite at circumneutral/basic PH conditions in electro-fenton processes, Catal. Today *361* (2021) 159–164, https://doi.org/10.1016/j.cattod.2020.03.027.

[51] Z. He, C. Gao, M. Qian, Y. Shi, J. Chen, S. Song, Electro-fenton process catalyzed by fe3o4 magnetic nanoparticles for degradation of C.I. reactive blue 19 in aqueous solution: operating conditions, influence, and mechanism, Ind. Eng. Chem. Res. *53* (2014) 3435–3447, https://doi.org/10.1021/ie403947b.

[52] H. Olvera-Vargas, X. Zheng, O. Garcia-Rodriguez, O. Lefebvre, Sequential "electrochemical peroxidation – electro-fenton" process for anaerobic sludge treatment, Water Res. *154* (2019) 277–286, https://doi.org/10.1016/j.watres.2019.01.063.

[53] Y. Li, S. Zhang, Y. Qin, C. Yao, Q. An, Z. Xiao, S. Zhai, Preparation of cobalt/hydrochar using the intrinsic features of rice hulls for dynamic carbamazepine degradation via efficient PMS activation, J. Environ. Chem. Eng. *10* (2022) 108659, https://doi.org/10.1016/j.jece.2022.108659.

[54] J. Cai, J. Xie, L. Xing, L. Zhou, Q. Zhang, M. Zhou, Enhanced mechanism of carbamazepine degradation by electrochemical activation of persulfate in flow-through system, Sep. Purif. Technol. *301* (2022) 122021, https://doi.org/10.1016/j.seppur.2022.122021.

[55] R. Zou, K. Tang, I. Angelidaki, H.R. Andersen, Y. Zhang, An innovative microbial electrochemical ultraviolet photolysis cell (MEUC) for efficient degradation of carbamazepine, Water Res. *187* (2020) 116451, https://doi.org/10.1016/j.watres.2020.116451.

[56] I. Kruusenberg, J. Leis, M. Arulepp, K. Tammeveski, Oxygen reduction on carbon nanomaterial-modified glassy carbon electrodes in alkaline solution, J. Solid State Electrochem. *14* (2010) 1269–1277, https://doi.org/10.1007/s10008-009-0930-2.